

Cite this: *RSC Adv.*, 2014, 4, 53795

Facile synthesis of gold nanoparticles using aggregates of pentacenequinone derivative and their catalytic activity for oxidative polymerization, homocoupling and reduction†

Kamaldeep Sharma, Vandana Bhalla* and Manoj Kumar

Received 24th September 2014
Accepted 13th October 2014

DOI: 10.1039/c4ra11116h

www.rsc.org/advances

The fluorescent aggregates of pentacenequinone derivative **3** serve as reactors for the preparation of gold nanoparticles through irreversible oxidative polymerization to furnish pentacenequinone based mesoporous polyaniline derivative. Further, gold nanoparticles so generated also exhibit excellent catalytic activity for conversion of phenyl boronic acid to biphenyl and reduction of nitro aromatics to amino derivatives.

1. Introduction

Gold nanoparticles (AuNPs) as green catalysts have generated great research interest in the frontiers between homogeneous and heterogeneous catalysis.¹ AuNPs and supported AuNPs have been used to catalyze various chemical transformations in organic synthesis such as photocatalytic hydroamination of alkynes and alkenes,² reduction of nitroaromatics³ and redox reactions.⁴ Keeping in view the importance of AuNPs, various methods such as seed mediated, chemical reduction, electrochemical, template based synthesis have been reported for the preparation of AuNPs. Most of these methods involve the use of reducing agents, stabilizing agents and shape directing additives.⁵ Further, the yield of AuNPs formed by these methods is also low. On the other hand, wet chemical method gives the high yield of metal nanoparticles of various shapes with control over their size and morphology,⁶ but this method suffers from the limitations of requiring longer reaction time and high temperature.⁷ Thus, development of a simple and facile method for the preparation of AuNPs with high catalytic efficiency remains a challenge. Recently, we reported pentacenequinone derivatives having nitrile groups.⁸ The fluorescent aggregates of these derivatives served as reactors for the preparation of gold nanoprisms and gold nanospheres. In continuation of this work, we now designed and synthesized symmetrically substituted pentacenequinone derivative **3** having amino groups at the periphery. We envisaged that aggregates of derivative **3** may exhibit affinity towards gold ions due to the presence of amino groups⁹ and will serve as reactors for the

preparation of AuNPs. To our pleasure, derivative **3** formed fluorescent aggregates in aqueous media and these aggregates served as reactors for the preparation of AuNPs without using any reducing and stabilizing agents at room temperature. Further, the gold nanoparticles so generated catalysed the oxidative polymerization of pentacenequinone derivative **3** which resulted in the formation of pentacenequinone based mesoporous polymeric material. The preparation of nitrogen rich porous materials has attracted a lot of research interest due to their potential applications in gas storage¹⁰ and as support for many important catalysts.¹¹ Interestingly, the nitrogen adsorption and desorption studies of the polyaniline derivative so obtained suggest that the material is mesoporous and was found to have Brunauer–Emmett–Teller (BET) surface area and adsorption average pore width of 5.0741 m² g^{−1} and 13.9 nm, respectively. Earlier, small molecules/polymers having amino groups have been used for preparation of gold nanoparticles¹² and in case of *o*-phenylenediamine, gold catalyzed oxidative polymerization of *o*-phenylenediamine monomers to poly(*o*-phenylenediamine)¹³ has been observed. However, there is no report regarding preparation of polymeric porous materials utilizing gold catalyzed oxidative polymerization. Various template based methods have been used for fabrication of porous materials.¹⁴ However, most of these methods require tedious post synthetic efforts for the removal of used template.¹⁵ In addition, removal of used template sometimes destroys the porous materials.¹⁶ Thus, development of a simple and facile method for the preparation of nitrogen rich porous material is an area of great interest. In the present manuscript, we report a simple and facile method for the preparation of AuNPs which catalyse the oxidative polymerization of pentacenequinone derivative **3**. To the best of our knowledge, this is the first report where gold catalyzed oxidative polymerization has been carried out for the preparation of pentacenequinone based mesoporous

Department of Chemistry, UGC Sponsored-Centre for Advanced Studies-I, Guru Nanak Dev University, Amritsar-143005, Punjab, India. E-mail: vanmanan@yahoo.co.in; Fax: +91 (0)183 2258820; Tel: +91 (0)183 22588029 ext. 3202

† Electronic supplementary information (ESI) available: Optical and spectroscopic data of derivatives **3**. See DOI: 10.1039/c4ra11116h

material. In addition, the AuNPs show good catalytic activity for the homocoupling of phenylboronic acid under aerobic conditions and reduction of nitroaromatics to amino derivatives. The catalytic activity of these NPs is better/comparable to reported systems in literature (see Table S1–S3 in ESI†).

2. Experimental section

2.1. Materials

All reagents were purchased from Aldrich and were used without further purification. THF was dried over sodium and benzophenone and kept over molecular sieves overnight before use. Silica gel (60–120 mesh) was used for column chromatography.

2.2. Instruments

UV-vis spectra were recorded on a SHIMADZU UV-2450 spectrophotometer, with a quartz cuvette (path length, 1 cm). The cell holder was thermostatted at 25 °C. The fluorescence spectra were recorded with a SHIMADZU 5301 PC spectrofluorimeter. Scanning electron microscope (SEM) images were obtained with a field-emission scanning electron microscope (SEM CARL ZEISS SUPRA 55). TEM images were recorded from Transmission Electron Microscope (TEM)-HITACHI. Elemental analysis (C, H, N) was performed on a Flash EA 1112 CHNS-O analyzer (Thermo Electron Corp.). ¹H NMR was recorded on a JEOL-FT NMR-AL 300 MHz spectrophotometer using CDCl₃ and DMSO-d₆ as solvent and tetramethylsilane SiMe₄ as internal standards. UV-vis studies were performed in THF and H₂O/THF mixture. Data are reported as follows: chemical shifts in ppm (δ), multiplicity (s = singlet, d = doublet, br = broad singlet m = multiplet), coupling constants *J* (Hz), integration, and interpretation.

2.3. Synthesis

Compound 3. To a solution of **1** (0.5 g, 0.808 mmol) and **2** (0.780 g, 3.56 mmol) in 1,4-dioxane (20 ml) were added K₂CO₃ (0.891 g, 6.464 mmol), distilled H₂O (2.1 ml) and [PdCl₂(PPh₃)₂] (0.170 g, 0.242 mmol) under N₂ atmosphere and the reaction mixture was refluxed overnight. The 1,4-dioxane was then removed under vacuum and the residue so obtained was treated with water, extracted with dichloromethane and dried over anhydrous Na₂SO₄. The organic layer was evaporated to dryness under reduced pressure and residue so obtained was purified by column chromatography using 95 : 5 (chloroform : MeOH) as an eluent to give 0.163 g (30%) of compound **3** as dark brown solid; mp. >260 °C; ¹H NMR (300 MHz, DMSO d₆): δ = 5.14 [s, 8H, NH₂], 6.49 [d, 8H, *J* = 6.0 ArH], 6.92 [d, 8H, *J* = 6.0 ArH], 8.15 [s, 4H, ArH], 8.86 [s, 4H, ArH], TOF MS ES+: 674.1713 (*M* + 2)⁺; elemental analysis: calcd. for C₄₆H₃₂N₄O₂: C 82.12; H 4.79; N 8.33; found: C 82.08; H 4.76; N 8.29. Due to poor solubility of compound **3** in common organic solvents, its ¹³C NMR spectrum could not be recorded.

Synthesis of AuNPs. To a 3 ml solution of compound **3** (10 μ M) in H₂O/THF (6 : 4, v/v) was added 0.1 M AuCl₃ (60 μ L). The reaction was stirred at room temperature for 2 min during

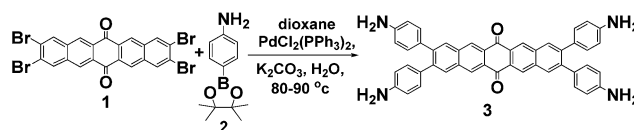
which the formation of AuNPs takes place. Solution of these NPs was used as such for the catalytic reactions.

3. Results and discussion

Pentacenequinone derivative **3** was synthesized by Suzuki-Miyaura coupling of 2,3,9,10-tetrabromopentacene 6,13-dione **1**¹⁷ with aniline boronic ester **2**¹⁸ (Scheme 1). The structure of derivative **3** was confirmed from its spectroscopic and analytical data. ¹H NMR spectrum of derivative **3** showed three singlets at 5.14, 8.15 and 8.86 ppm, two doublets at 6.49 and 6.92 ppm corresponding to the NH₂ and aromatic protons, respectively (Fig. S18 in ESI†). The mass spectrum of derivative **3** showed a parent ion peak at *m/z* 674.1713 (*M* + 2)⁺ (Fig. S19 in ESI†). These spectroscopic data corroborate the structure **3** for this compound.

The UV-vis spectrum of derivative **3** in THF exhibits two absorption bands at 287 and 415 nm, respectively. On addition of water (\leq 60% volume fractions) to the THF solution of derivative **3**, the absorption band at 415 is blue shifted to 396 nm and level-off tail is observed in the visible region (Fig. 1A). The absorption studies suggest the formation of aggregates in the aqueous media. On the other hand, in the fluorescence spectrum, aggregates of derivative **3** in H₂O/THF (6 : 4) exhibit two emission bands at 373 and 477 nm (Fig. S2 in ESI†) which result from locally excited state and intramolecular charge transfer state, respectively.¹⁹ The scanning electron microscopy (SEM) image of derivative **3** in the solvent mixture of H₂O/THF (6 : 4) shows the presence of irregular shaped aggregates (Fig. 1B). The aggregates formed were visibly transparent and stable at room temperature for several weeks.

The presence of amino groups at the periphery of the derivative **3** prompted us to investigate its sensing behaviour toward different metal ions by UV-vis and fluorescence spectroscopy. The UV-vis studies of aggregates of derivative **3** (10 μ M) in H₂O/THF (6 : 4) mixture were carried out toward different metal ions such as Au³⁺, Ag⁺, Ni²⁺, Cu²⁺, Cd²⁺, Hg²⁺, Fe²⁺, Zn²⁺, Pb²⁺, Fe³⁺, Co²⁺, Na⁺, K⁺, Li⁺, Cr³⁺ ions as their perchlorate/chloride/or both perchlorate and chloride salts. Among various metal ions tested, nanoaggregates of derivative **3** show selective response towards Au³⁺ ions (Fig. S3 and S4 in ESI†). Upon addition of Au³⁺ ions (200 equiv.) to the solution of derivative **3** in mixed aqueous media (H₂O/THF, 6/4), a new absorption band is observed at 560 nm which suggests the formation of AuNPs (inset Fig. 2A).²⁰ The intensity of this band increases with time and the rate constant²¹ for the formation of AuNPs was found to be $7.18 \times 10^{-5} \text{ s}^{-1}$ (see pS12 in ESI†).²² On the other hand, complete quenching in fluorescence intensity



Scheme 1 Synthesis of pentacenequinone derivative **3**.

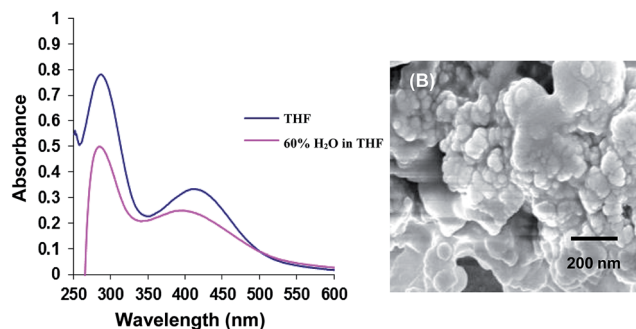


Fig. 1 (A) UV-vis spectra of derivative **3** (10 μ M) showing the variation of absorption intensity in THF and 60% H_2O /THF mixture (B) SEM image of derivative **3** in H_2O /THF (6 : 4) mixture showing irregular shaped aggregates; scale bar 200 nm.

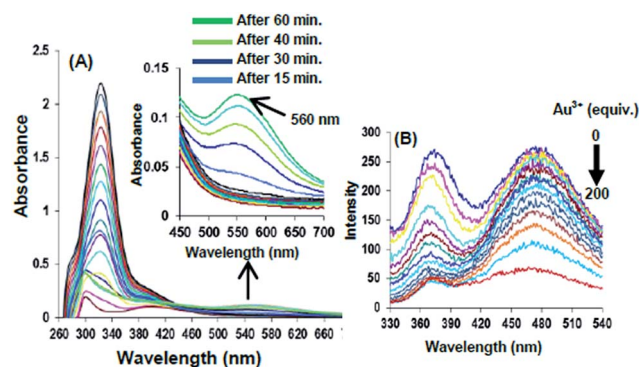


Fig. 2 (A) UV-vis spectra of derivative **3** (10 μ M) upon addition of Au^{3+} ions (200 equiv.) and at different time intervals in H_2O /THF (6/4) inset: UV-vis spectra in range 450–700 nm taken at different time intervals showing band at 560 nm. (B) Fluorescence spectra of derivative **3** (10 μ M) upon addition of Au^{3+} ions in H_2O /THF (6/4); buffered with HEPES, pH = 7.0. $\lambda_{\text{ex.}}$ = 287 nm.

was observed upon addition of Au^{3+} ions (0–200 equiv.) to the solution of derivative **3** (H_2O /THF, 6/4) (Fig. 2B). This quenching in fluorescence emission is attributed to binding of Au^{3+} ions with nanoaggregates of derivative **3**. The changes in the absorption spectra suggest interaction of gold ions with the amino groups of aggregates of derivative **3** and their subsequent reduction to zero valent gold atoms.

The detection limit for Au^{3+} ions was found to be 70 nM (70×10^{-9} M). The calculated Stern–Volmer constant of nanoaggregates of derivative **3** for Au^{3+} ions was found to be $1.63 \times 10^3 \text{ M}^{-1}$ (Fig. S6 in ESI†). Under the same conditions as used for Au^{3+} ions, we tested the binding behaviour of aggregates of derivative **3** toward other metal ions such as Au^{3+} , Ag^+ , Ni^{2+} , Cu^{2+} , Cd^{2+} , Hg^{2+} , Fe^{2+} , Zn^{2+} , Pb^{2+} , Fe^{3+} , Co^{2+} , Na^+ , K^+ , Li^+ , Cr^{3+} ions (Fig. S7 and S8 in ESI†) but no significant change in fluorescence intensity of aggregates of derivative **3** was observed (Fig. S9 in ESI†).

The TEM images of solution of derivative **3** in the presence of gold ions show the presence of bundles of nanofibres and spherical AuNPs (Fig. 3A and B).

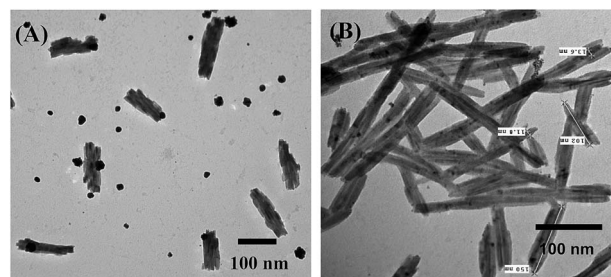


Fig. 3 TEM images of aqueous gold solution of derivative **3** showing presence of bundles of nanofibres and spherical gold nanoparticles. Scale bar (A) and (B) 100 nm.

The presence of peaks of Au, C, O and N in energy dispersive X-ray (EDX) spectrum of resulting solution (Fig. S10 in ESI†) confirmed the presence of organic compound and AuNPs.¹³

To get insight into the mechanism of formation of AuNPs and polyaniline material, we slowly evaporated the solution of aggregates of derivative **3** containing AuNPs. After several days, precipitates were observed. The X-ray diffraction (XRD) analysis of the resulting precipitates showed the broad peak centered at Bragg angle ($2\theta/\text{degree}$) $\sim 24^\circ$ which may be attributed to amorphous polyaniline polymer.¹³ Further, four diffraction peaks were observed at 37.82 , 44.08 , 64.28 , and 77.24° which may be assigned to 111, 200, 220 and 311 faces of a Au crystal, respectively (Fig. S11 in ESI†). These four peaks showed the characteristic pattern of face-centered cubic (fcc) gold (0).²³ Next, the precipitates were washed several times with THF. The ^1H NMR spectrum of the residue so obtained after evaporation of THF exhibits three sharp peaks at 6.93, 7.05 and 7.14 ppm corresponding to $-\text{NH}_2$ and $-\text{NH}-$ groups²⁴ of polyaniline derivative (see pS21 in ESI†). Thus, ^1H NMR study supports the formation of pentacenequinone based polyaniline derivative. The SEM images of resulting residue show presence of entangled nanorods with network structure (Fig. 4A–C).

The porous structure of polyaniline was characterized by atomic force microscopy (AFM) through non-contact measurements. The topography images of polyaniline (Fig. 5) show porous surface.

The porosity parameters of polyaniline were studied by using nitrogen adsorption and desorption measurements to determine the pore size and specific surface area of the polymeric material (Fig. 6).

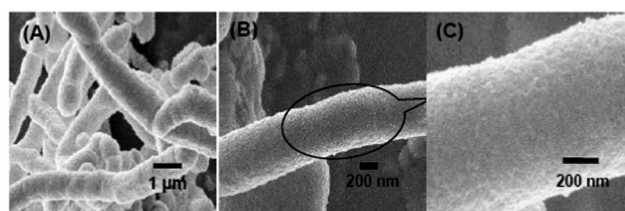


Fig. 4 SEM images of pentacenequinone based polyaniline obtained after oxidative polymerization of derivative **3**. Scale bar (A) 1 μ m (B) and (C) 200 nm.

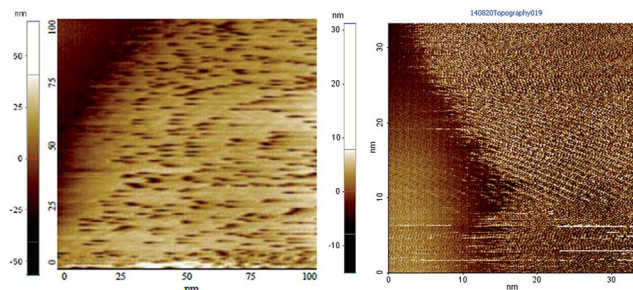


Fig. 5 Topographical AFM-images of the surface of polyaniline of derivative 3 showing presence of pores.

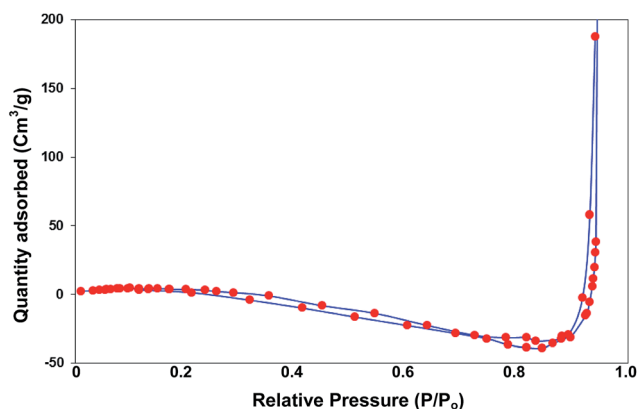
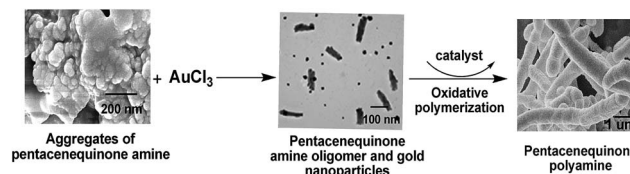


Fig. 6 Nitrogen adsorption and desorption curve of polyaniline of derivative 3 at 295 K.

The Brunauer–Emmett–Teller (BET) study shows presence of pores of size 13.9 nm with B.E.T surface area of 5.074 ($\text{m}^2 \text{g}^{-1}$). The negative values of the adsorbed quantity reveal that tubular polyaniline structure has almost no micropores.²⁵ The nitrogen adsorption and desorption data at 275 K is given in Table 1.

We also carried out UV-vis studies of derivative 3 towards Au^{3+} ions in pure THF. However, absorption spectrum does not indicate formation of nanoparticles (Fig. S12 in ESI†). These studies suggest the importance of water in the preparation of AuNPs. We propose that upon addition of Au^{3+} ions to the solution of aggregates of 3, the gold ions enter the network of interconnected channels, interact with amino groups and get reduced. Thus, aggregates of derivative 3 function as reducing agent as well as stabilizing agent for the preparation of AuNPs.²⁶ Further, the AuNPs so generated catalyze the oxidative polymerization of derivative 3, hence, polyaniline of derivative 3 was obtained (Scheme 2).



Scheme 2 Schematic diagram to illustrate the probable reaction mechanism for the formation of polyaniline.

We also investigated the catalytic activity of the AuNPs so generated in the aqueous media for the homocoupling of phenylboronic acid under aerobic conditions (See pS7 in ESI†). We were pleased to know that in comparison to reported systems, AuNPs of derivative 3 exhibit better/comparable catalytic activity for the homocoupling of phenylboronic acid under aerobic conditions (See pS4 in ESI†). In a toluene/ H_2O (2 : 1) mixture, the yield of biphenyl and phenol in the products was found to be 80% and 20%, respectively. Further, we also investigated the reduction of *p*-nitroaniline and *p*-nitrophenol to *p*-phenylenediamine and *p*-aminophenol in the presence of AuNPs using NaBH_4 (see pS8 in ESI†). Addition of catalytic amount of gold nanoparticles solution 5 μL (10 nmol) generated by aggregates of derivative 3 to the solution of *p*-nitroaniline and *p*-nitrophenol results in complete reduction of *p*-nitroaniline and *p*-nitrophenol to *p*-phenylenediamine and *p*-aminophenol in 18 minutes and 8 minutes respectively (Fig. 7A and B).

The reaction was monitored by UV-vis spectroscopy and the calculated rate constants²¹ for the catalytic reduction of *p*-nitroaniline and *p*-nitrophenol by gold nanoparticles of derivatives 3 were found to be $4.53 \times 10^{-3} \text{ s}^{-1}$ and $8.85 \times 10^{-3} \text{ s}^{-1}$, respectively (see pS18 in ESI†). A blank experiment was carried out for the reduction of *p*-nitroaniline and *p*-nitrophenol with

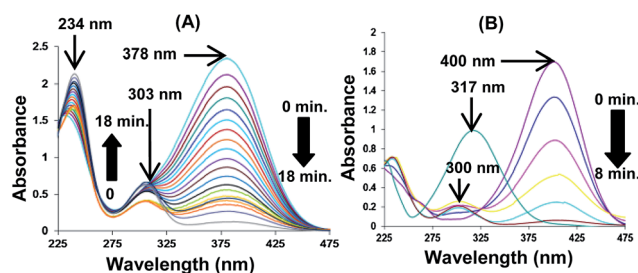


Fig. 7 UV-vis spectra for the reduction of (A) *p*-nitroaniline and (B) *p*-nitrophenol by adding NaBH_4 aqueous solution using gold nanoparticles of derivative 3 as catalyst.

Table 1 Surface area, pore size, pore volume, and N_2 adsorbed for polyaniline material

Material	BET surface area ($\text{m}^2 \text{g}^{-1}$)	Langmuir surface area ($\text{m}^2 \text{g}^{-1}$)	Pore volume ($\text{cm}^3 \text{g}^{-1}$)	Adsorption average pore width (nm)	Volume of N_2 adsorbed $\text{cm}^3 \text{g}^{-1}$
Polyaniline	5.0741	20.2870	0.053714	13.9	3.33

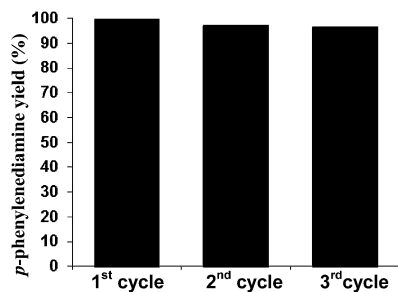


Fig. 8 Recyclability of the AuNPs catalyst for the reduction of *p*-nitroaniline with NaBH₄.

NaBH₄ in the absence of AuNPs. There is a very slow decrease in the characteristic absorbance of *p*-nitroaniline and *p*-nitrophenol after 24 h (Fig. S14 and S15 in ESI†).

The catalytic reduction of *p*-nitroaniline to *p*-phenylenediamine in the presence of NaBH₄ aqueous solution was chosen as a model reaction to investigate the reusability of AuNPs catalyst. In the first cycle, the product *p*-phenylenediamine was obtained in quantitative yield with complete conversion of *p*-nitroaniline. The resulting reaction mixture containing AuNPs catalyst was subjected to reaction for the next catalytic sequence by adding *p*-nitroaniline and NaBH₄. The AuNPs could be re-used as a catalyst for the catalytic reduction reaction at least seven times (Fig. S16 in ESI†).²⁷ Further, recyclability of heterogeneous AuNPs catalyst was checked by using same reaction.²⁸ The AuNPs catalyst could be precipitated after the reaction by addition of dichloromethane to the reaction mixture, filtered and reused at least three times using this recycling procedure for identical reactions. The reaction yield remained quantitative or almost so upon these three recycling reactions (resp. 99.6%, 97%, 96.5%) (Fig. 8).

4. Conclusion

We designed and synthesized symmetrically substituted pentacenequinone derivative **3** which forms aggregates in aqueous media. These aggregates serve as reactors for preparation of AuNPs. AuNPs so generated act as catalyst for preparation of mesoporous polyaniline derivative. In addition, AuNPs also exhibit efficient catalytic activity towards homocoupling reaction of phenylboronic acid in aerobic conditions and reduction of nitro aromatics to amino derivatives.

Acknowledgements

V. B. is thankful to CSIR (ref. no. 02(0083)/12/EMR-II). M. K. is thankful to DRDO [(ref. no. ERIP/ER/1003922/M/01/1429)]. We are thankful to UGC (New Delhi, India) for the "University with Potential for Excellence" (UPE) project. K. D. S is thankful to DST-PURSE for fellowship. We are thankful to Shahi Imam Reja for helpful discussions.

Notes and references

- (a) D. Astruc, F. Lu and J. R. Aranzas, *Angew. Chem., Int. Ed.*, 2005, **44**, 7852; (b) M. C. Daniel and D. Astruc, *Chem. Rev.*, 2004, **104**, 293.
- (a) A. S. K. Hashmi, R. Salathe and W. G. Frey, *Synlett*, 2007, 1763; (b) N. Nishina and Y. Yamamoto, *Synlett*, 2007, 1767; (c) R. L. LaLonde, B. D. Sherry, E. J. Kang and F. D. Toste, *J. Am. Chem. Soc.*, 2007, **129**, 2452; (d) T. E. Müller, M. Grosche, E. Herdtweck, A. K. Pleier, E. Walter and Y. K. Yan, *Organometallics*, 2000, **19**, 170.
- (a) J. Guo and K. S. Suslick, *Chem. Commun.*, 2012, **48**, 11094; (b) R. Liu, S. M. Mahurin, C. Li, R. R. Unocic, J. C. Idrobo, H. Gao, S. J. Pennycook and S. Dai, *Angew. Chem., Int. Ed.*, 2011, **50**, 6799.
- (a) M. M. Maye, N. N. Kariuki, J. Luo, L. Han, P. Njoki, L. Wang, Y. Lin, H. R. Naslund and C. Zhong, *Gold Bull.*, 2004, **37**, 217; (b) S. Schimpf, M. Lucas, C. Mohr, U. Rodemerck, A. Brückner, J. Radnik, H. Hofmeister and P. Claus, *Catal. Today*, 2002, **72**, 63.
- N. Li, P. Zhao and D. Astruc, *Angew. Chem., Int. Ed.*, 2014, **53**, 1756.
- A. M. Alkilany and C. J. Murphy, *Langmuir*, 2009, **25**(24), 13874.
- X. Sun, X. Jiang, S. Dong and E. Wang, *Macromol. Rapid Commun.*, 2003, **24**, 1024.
- K. Sharma, S. Kaur, V. Bhalla, M. Kumar and A. Gupta, *J. Mater. Chem. A*, 2014, **2**, 8369.
- (a) M. J. Rak, N. K. Saadé, T. Friščić and A. Moores, *Green Chem.*, 2014, **16**, 86; (b) X. Yang, L. Gan, L. Han, D. Li, J. Wang and E. Wang, *Chem. Commun.*, 2013, **49**, 2302.
- (a) D. E. Demircak, M. K. Ram, S. S. Srinivasan, D. Y. Goswami and E. K. Stefanakos, *J. Mater. Chem. A*, 2013, **1**, 13800; (b) K. Jurewicz, K. Babel, A. Ziolkowski and H. Wachowska, *Electrochim. Acta*, 2003, **48**, 1491.
- M. K. Bhunia, S. K. Das, P. Pachfule, R. Banerjee and A. Bhaumik, *Dalton Trans.*, 2012, **41**, 1304.
- (a) Y. Xia, Y. Xiong, B. Lim and S. E. Skrabalak, *Angew. Chem., Int. Ed.*, 2009, **48**, 60; (b) X. Sun, S. Dong and E. Wang, *Angew. Chem., Int. Ed.*, 2004, **43**, 6360.
- X. P. Sun, S. J. Dong and E. K. Wang, *Chem. Commun.*, 2004, 1182.
- (a) H. Nishihara and T. Kyotani, *Adv. Mater.*, 2012, **24**, 4473; (b) H. L. Jiang, B. Liu, Y. Q. Lan, K. Kuratani, T. Akita, H. Shioyama, F. Q. Zong and Q. Xu, *J. Am. Chem. Soc.*, 2011, **133**, 11854; (c) Y. Xia, Z. Yang and R. Mokaya, *Nanoscale*, 2010, **2**, 639.
- J. Huang and R. B. Kaner, *J. Am. Chem. Soc.*, 2004, **126**, 851.
- Z. Wei, Z. Zhang and M. Wan, *Langmuir*, 2002, **18**, 917.
- C. R. Swartz, S. R. Parkin, J. E. Bullock, J. E. Anthony, A. C. Mayer and G. G. Malliaras, *Org. Lett.*, 2005, **7**, 3163.
- V. Bhalla, R. Tejpal, M. Kumar, R. K. Puri and R. K. Mahajan, *Tetrahedron Lett.*, 2009, **50**, 2649.
- S. I. Druzhinin, S. A. Kovalenko, T. A. Senyushkina, A. Demeter and K. A. Zachariasse, *J. Phys. Chem. A*, 2010, **114**, 1621.

- 20 T. Serizawa, Y. Hirai and M. Aizawa, *Langmuir*, 2009, **25**, 12229.
- 21 S. Goswami, S. Das, K. Aich, D. Sarkar, T. K. Mondal, C. K. Quah and H.-K. Fun, *Dalton Trans.*, 2013, **42**, 15113.
- 22 (a) T. K. Sau and C. J. Murphy, *Langmuir*, 2004, **20**, 6414; (b) N. R. Jana, L. Gearheart and C. J. Murphy, *Chem. Mater.*, 2001, **13**, 2313.
- 23 M. Amin, F. Anwar, M. R. S. A. Janjua, M. A. Iqbal and U. Rashid, *Int. J. Mol. Sci.*, 2012, **13**, 9923.
- 24 (a) M.-R. Huang, X.-G. Li and Y. Yang, *Polym. Degrad. Stab.*, 2001, **71**, 31; (b) X.-G. Li, M.-R. Huang and Y. Yang, *Polymer*, 2001, **42**, 4099.
- 25 W. Wu, X. H. Xiao, S. F. Zhang, T. C. Peng, J. Zhou, F. Ren and C. Z. Jiang, *Nanoscale Res. Lett.*, 2010, **5**, 1474.
- 26 (a) X. Sun, X. Jiang, S. Dong and E. Wang, *Macromol. Rapid Commun.*, 2003, **24**, 1024; (b) M. N. Nadagouda and R. S. Varma, *Green Chem.*, 2008, **10**, 859.
- 27 Y. Isomura, T. Narushima, H. Kawasaki, T. Yonezawa and Y. Obora, *Chem. Commun.*, 2012, **48**, 3784.
- 28 V. Reddy, R. S. Torati, S. Oh and C. Kim, *Ind. Eng. Chem. Res.*, 2013, **52**, 556.